Composites: Part A 39 (2008) 1915–1923

Contents lists available at ScienceDirect

Composites: Part A

journal homepage: www.elsevier.com/locate/compositesa

Strengthening of polypropylene–glass fiber interface by direct metallocenic polymerization of propylene onto the fibers

Mariana Etcheverry [a], María L. Ferreira [a], Numa J. Capiati [a], Alessandro Pegoretti [b], Silvia E. Barbosa [a,*]

[a] PLAPIQUI (UNS-CONICET) Camino "La Carrindanga" Km. 7, 8000 Bahía Blanca, Argentina
[b] University of Trento Department of Materials Engineering, Via Mesiano 77, 38100 Trento, Italy

ARTICLE INFO

Article history:
Received 26 May 2008
Received in revised form 17 September 2008
Accepted 26 September 2008

Keywords:
B. Adhesion
B. Interface/interphase
B. Fragmentation
In situ polymerization

ABSTRACT

This work deals with the development of a new approach to improve the interfacial adhesion and properties of polypropylene–glass fiber composites. The chemical anchoring of the matrix polymer on glass fibers was improved by direct metallocenic polymerization of propylene onto the fibers surface. The experimental route involves an initial contact with methylaluminoxane (MAO) and hydroxy-α-olefin to generate the anchorage points on the fiber surface, followed by a propylene polymerization catalyzed by $EtInd_2ZrCl_2$ (metallocene)/MAO. During the polymerization reaction, polypropylene chains grow on the glass fiber surface. This reaction was studied for different hydroxy-α-olefin concentrations and its effectiveness was characterized by scanning electron microscopy (SEM) with X-ray disperse energy microanalysis. An evaluation of the fiber–matrix interfacial shear strength (ISS) was performed by single-fiber fragmentation tests on model composites. Depending on the hydroxy-α-olefin concentration, the surface treatment induced an increase of the ISS with respect of the untreated fibers by a factor ranging from 1.7 up to 2.1. The improved interfacial adhesion level was also confirmed by SEM observations of the morphology of the fiber–matrix region of cryogenic-fractured surfaces of composites.

1. Introduction

Even if polymer composites have been used for thousands of years, it has only been during the last half century that applications have become so demanding that the tailoring of well-bonded, durable interfaces between the matrix and reinforcement has become a critical issue. The use of coupling agents, chemically reactive with matrix and reinforcement, and/or surface physicochemical modifications of one or both constituents have been proven to be the most successful means to improve the bonding between matrix and reinforcement [1–5].

It is widely known that silane-coupling agents increase ultimate mechanical properties, whereas titanate coupling agents may improve processability and flexibility. The former are particularly effective for silicon-based fillers and the latter can be applied to a variety of fibers. Nevertheless, the coupling mechanism of these agents has not been fully clarified, probably because of the complex nature of the interfacial interactions [1,5].

Many years of research have been invested in characterizing the molecular structure of the interphase region and its relation to mechanical and chemical stability. In particular, the mechanical properties of fiber reinforced composites are strongly dependent upon the stability of the interfacial region. On the other hand, the adhesion between phases can be easily degraded in aggressive environmental conditions such as high temperature and/or elevated moisture, and by the state of stress to which the material is exposed. This is of particular importance in glass fiber reinforced materials since they are mostly used in industrial applications involving an extended exposure to water, as for components used in marine or transportation fields. Thus, the water accumulated at unprotected glass fiber surfaces, over a period of time, can cause both a loss of adhesion and a reduction in fiber strength. Under usual service conditions, individual filaments will fracture at lower loads than the initial fiber strength, thus behaving as precursors of critical levels of damage. When a filament fractures, the stored elastic energy lost by the constituents, in the region around the broken fiber ends, is sufficient to propagate cracks into the matrix and/or along the interface [6,7]. The precise mode of failure is a function of the environmental conditions and time, thus complicating prediction on long-term behavior [2].

Many studies have focused to the development of reliable experimental test procedures to determine the fiber–matrix interfacial strength [8–10]. The most common methods are based on micromechanical tests performed on single fiber composites, such as the fragmentation test [11–16], the single fiber pull-out test [17,18], the microdebonding test [19–22], and the microindentation test [23–25]. Probably the method most widely used to characterize the composites interface is the fragmentation of a single fiber embedded in the polymer matrix [13,26]. According to this

* Corresponding author. Tel.: +54 291 4861700x271; fax: +54 291 4861600.
E-mail address: sbarbosa@plapiqui.edu.ar (S.E. Barbosa).

1359-835X/$ - see front matter © 2008 Elsevier Ltd. All rights reserved.
doi:10.1016/j.compositesa.2008.09.018

approach, a tensile load is applied to a model composite consisting of a single filament embedded in a polymeric matrix longitudinally to the loading direction. As the strain increases, the filament fails prior to the matrix due to its much lower strain-to-break. The fragmentation process continues and the filament breaks repeatedly until the stress transferred through the interface is no longer enough to induce further ruptures. At this point the fragments reach a critical length (L_c) which characterizes the interfacial shear strength. A rigorous treatment of the fragmentation test process requires consideration of the complex interfacial state of stress [10,12–16], as well as a careful statistical analysis in order to avoid errors due to extrapolation of the fiber strength to very small lengths [27–29].

In this work, a new approach to increase the adhesion between polypropylene (PP) and glass fiber (GF) based on polymerization of propylene directly onto the fibers surface is explored. The chemical anchoring of PP on glass fibers by direct metallocenic polymerization was reported previously [30,31]. The experimental route involves an initial contact with methylaluminoxane (MAO) and a hydroxy-α-olefin to generate the anchorage points on the fiber surface, followed by the propylene polymerization catalyzed by $EtInd_2ZrCl_2$ (metallocene)/MAO. As a result, PP chains grow from the glass fiber surface.

The present paper is focused on the assessment of the effects of this polymer layer on the PP–GF adhesion for different hydroxy-α-olefin concentrations. The effectiveness of this reaction was characterized by scanning electron microscopy with on line X-ray disperse energy microanalysis (SEM/EDX). The adhesion measurements were performed by the single-fiber fragmentation test. The morphology of cryogenic-fracture surfaces of model composites was also analyzed by SEM.

2. Theoretical background on the fragmentation tests

According to the Kelly–Tyson approach [12] the average value of interfacial shear strength (ISS) is the result of the static equilibrium between the tensile force acting on a fiber and the shear force transferred through the fiber–matrix interface [13,32]:

$$\mathrm{ISS} = \frac{\sigma_{\mathrm{fb(Lc)}} d}{2L_c} \tag{1}$$

where d is the fiber diameter and $\sigma_{\mathrm{fb(Lc)}}$ is the tensile strength of a fiber with a critical length L_c. The value of the critical fragment length can be determined from the average length at saturation (L_s), assuming that the distribution of the fiber fragment lengths, at the end of the rupture process, is quasi-symmetrical:

$$L_c = \frac{4}{3} L_s \tag{2}$$

It is clear, from Eq. (1), that the calculation of ISS implies to know how the fiber strength depends on the fiber length. In the present work, this relation was experimentally assessed by carrying out single filament tensile tests following ASTM 3379 standard [33]. These tests were conducted at a given gauge length and the data were fitted by a two-parameter Weibull distribution. According to the 'weakest link' approximation, it is assumed that a fiber of length L is formed by N independent links of arbitrary unit length L_0, each link failing or surviving at a given stress level, independently of its neighbors. The strength distribution of each link is also described by a simple Weibull distribution, characterized by identical shape parameter. Then, the Weibull cumulative distribution function $F(\sigma)$, and the corresponding average strength, $\sigma_{\mathrm{fb(L)}}$, are, respectively, given by:

$$F(\sigma) = 1 - \exp\left[-L\left(\frac{\sigma}{\sigma_0}\right)^m\right] \tag{3}$$

and

$$\sigma_{\mathrm{fb}}(L) = \sigma_0 \left(\frac{L}{L_0}\right)^{-\frac{1}{m}} \Gamma\left(1 + \frac{1}{m}\right) \tag{4}$$

where Γ is the Gamma function.

The scale (σ_0) and shape (m) parameters of the Weibull distribution were estimated from strength data determined at one single gauge length by fitting the distribution of failure probability. The fiber tensile strength at any gauge length needed for the calculation of ISS was finally calculated on the basis of Eq. (4).

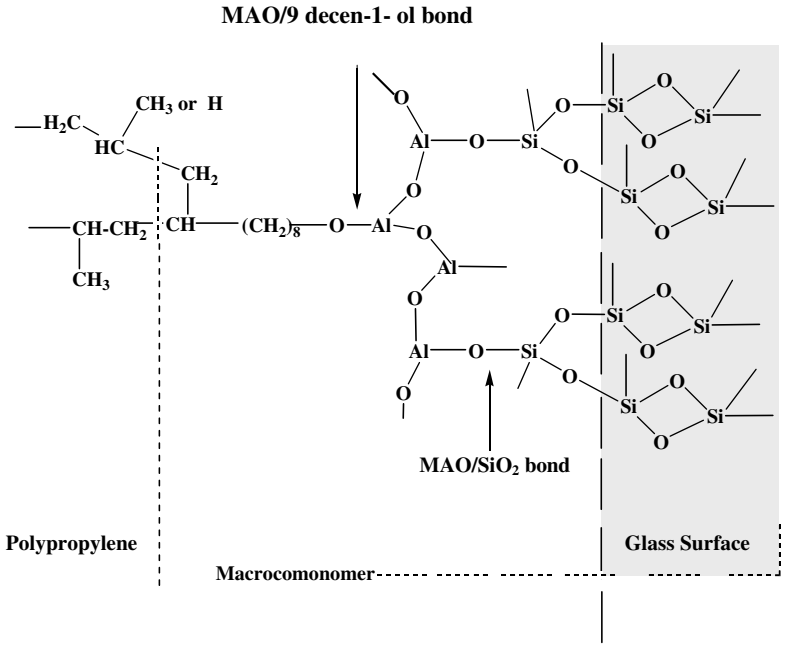

Fig. 1. Chemical species bonded onto the glass fiber.

3. Experimental

3.1. Materials

The polymerization grade propylene, the cocatalyst 9 decen-1-ol, and the metallocene catalyst ($EtInd_2ZrCl_2$) for in situ polymerization were supplied by Sigma–Aldrich. The MAO was furnished by Witco. The reaction was performed onto E-glass monofilaments of 20 μm diameter supplied by Vetrotex Argentina, and toluene (HPLC purity) from J.T. Baker was used as solvent.

For the preparation of microcomposite samples, a commercial PP film supplied by MG Lavorazioni Materie Plastiche (Vicenza,

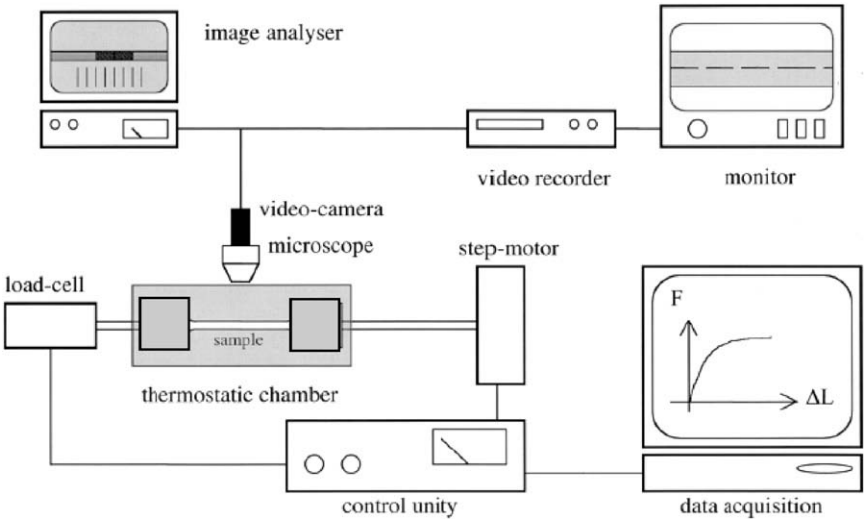

Fig. 2. Single fiber fragmentation test set up.

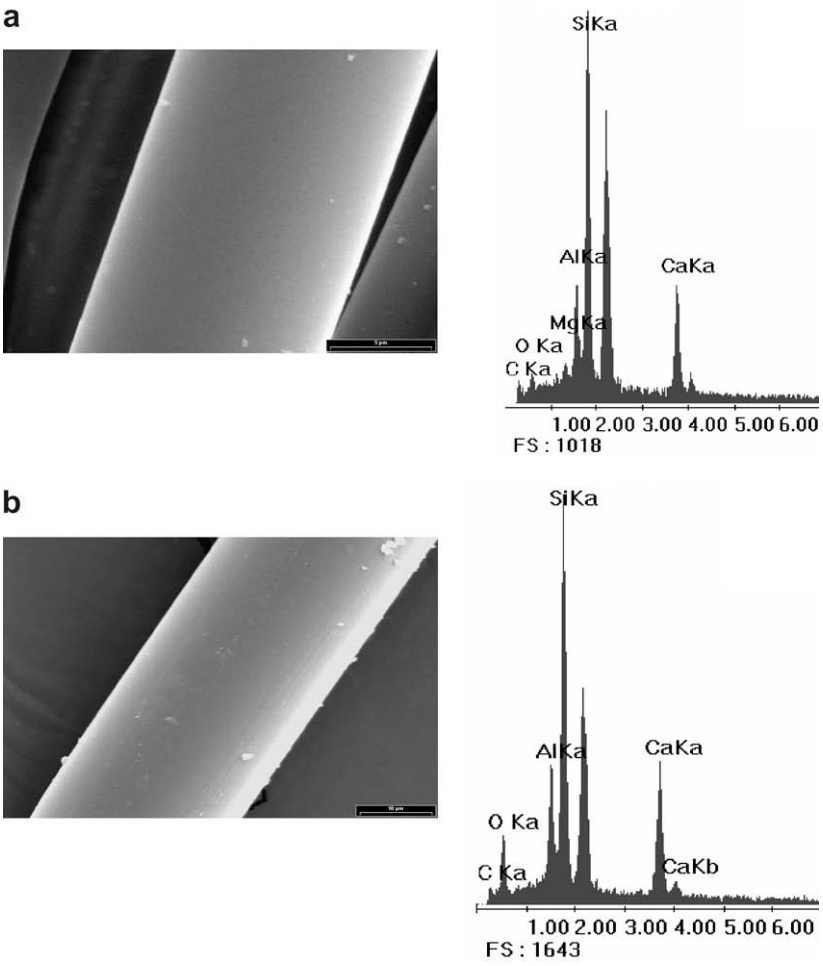

Fig. 3. SEM microphotographs and the correspondent EDX spectra for: (a) untreated fibers (6000×) and (b) MAO treated fibers (2000×).

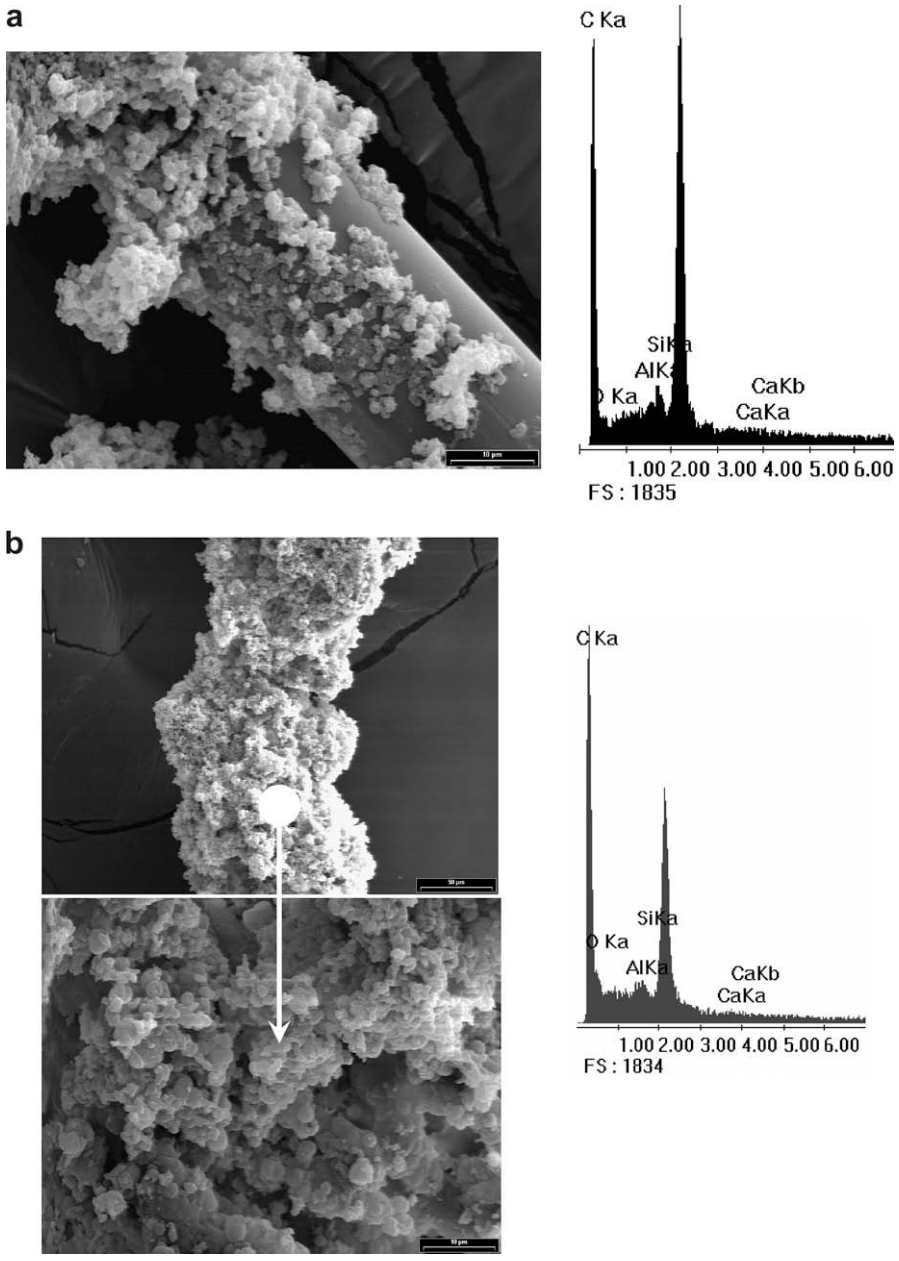

Fig. 4. SEM microphotographs (2000×) and the correspondent EDX spectra for polymerized fibers with different amounts of hydroxy-α-olefin: (a) 0.5%, (b) 1.0% (include a 400× magnification), (c) 1.5%, and (d) 2.0%.

Italy) was used. This film had a nominal thickness of 78 μm and was obtained from a polypropylene co-ethylene random copolymer (Moplen RP348T from Basell) with ethylene content lower than 4%.

3.2. In situ polymerization reaction

Reactions were performed in a 300 ml stainless steel stirred reactor. Fibers were perfectly aligned parallel each other and supported on a special glass frame, in order to expose their entire surface to the reactants. The reactor, with fibers and 260 ml of toluene, was flushed out with propylene for 30 min. Then, different concentrations of 9 decen-1-ol, MAO and 1 mg of metallocene were added. The polymerization reaction was carried out during 45 min at 65 °C. Four concentrations of hydroxy-α-olefin (0.5, 1.0, 1.5 and 2.0 mol% of hydroxyl content) were used. These concentrations are related to the concentration of propylene in toluene at the reaction temperature and 1 atm [34]. The MAO/9 decen-1-ol ratio was about 100/1 by volume in order to assure an excess of MAO in the reactor. The reaction scheme is schematically reported in Fig. 1. After reaction occurrence, a mixture of ethanol/hydrochloric acid was added to precipitate the polymer from the solution. Then, the fibers were washed with distilled water and separated from the frame. Detailed information of the reaction technique is reported elsewhere [30,31].

3.3. Mechanical tests

3.3.1. Fiber strength

The mechanical strength of individual fibers was determined by an Instron 4502 tensile tester equipped with a 10 N load cell according to the test procedure described by the ASTM C-1557-

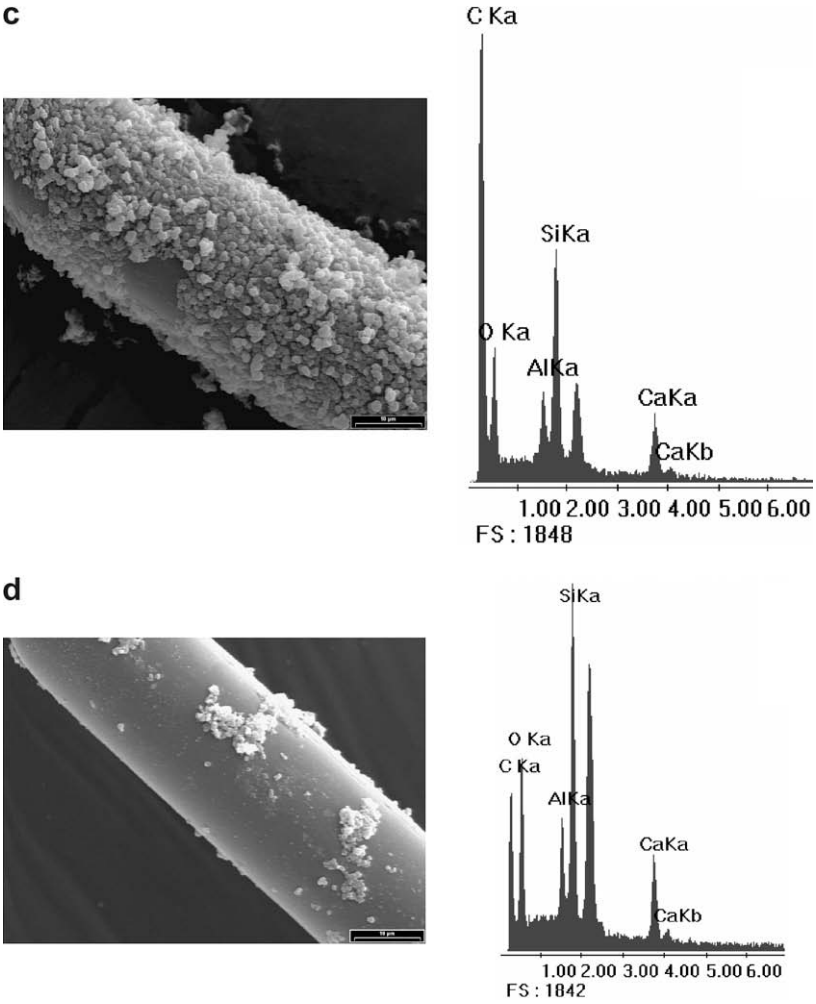

Fig. 4 (*continued*)

03 standard. The gage length was fixed at 25 mm and the cross-head speed was 1 mm/min. Tests were performed on both untreated (34 specimens) and MAO-treated (34 specimens) glass fibers. The last set of specimens was prepared following the reaction procedure described above, but using only MAO on the fiber surface, in order to check its effect on the fiber strength. Fiber diameters were determined by optical microscopy.

3.3.2. Interfacial shear strength evaluation

The interfacial adhesion was determined by single fiber fragmentation tests, carried out on model composites consisting of a single glass fiber embedded in a PP matrix. Microcomposite samples were prepared by compression molding. Fibers were carefully aligned between two PP films, in turn sandwiched between two stainless steel sheets. The mold was placed in a vacuum oven at 165 °C, under a constant pressure at 7 kPa for about 20 min, and then cooled to room temperature. Samples were obtained by cutting rectangular strips containing a fiber straightly aligned in the middle axis. The microcomposites dimensions were roughly 0.16 mm in thickness, 5 mm in width and 25 mm in length. Samples were prepared using untreated and treated fibers with 0.5%, 1.0%, 1.5% and 2.0% of hydroxy-α-olefin, and they were named M0.0, M0.5, M1.0, M1.5 and M2.0, respectively.

Single fiber fragmentation tests were performed at room temperature and at a cross-head speed of 1 mm/min by using a custom-made apparatus as shown in Fig. 2. This device consists of a

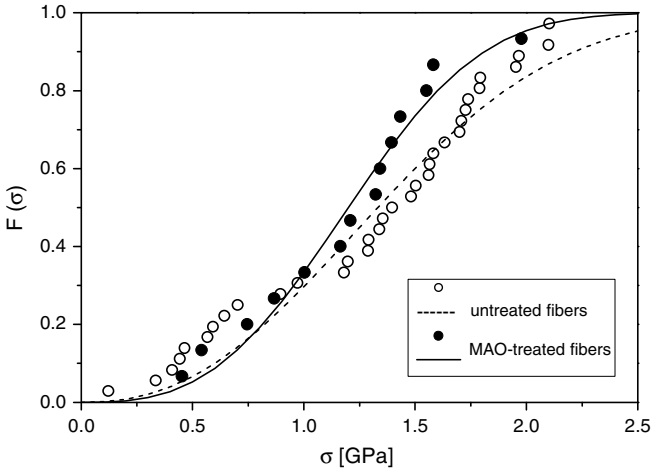

Fig. 5. Weibull plot of untreated (○) and MAO-treated (●) fibers.

Table 1
Weibull scale and shape parameters for a reference length $L_0 = 25$ mm.

	Scale parameter, σ_0 (MPa)	Shape parameter, m	χ^2	R
Untreated fibers	1556 ± 24	2.36 ± 0.17	0.122	0.976
MAO-treated fibers	1361 ± 22	2.92 ± 0.25	0.029	0.986

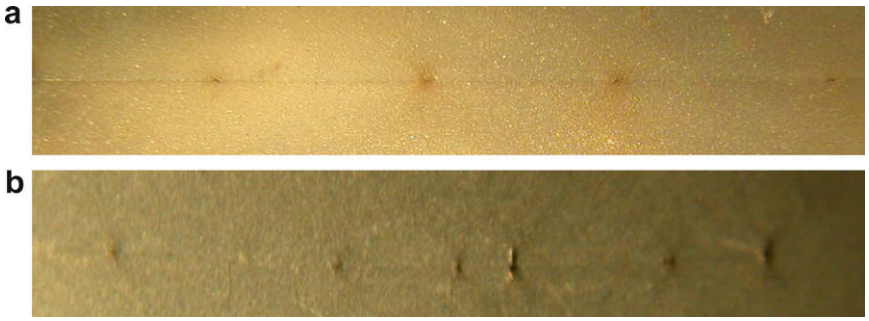

Fig. 6. Optical microphotograps (4×) from fragmented fiber in microcomposites (a) M0.0 and (b) M1.0.

Table 2
Average fiber critical length, L_c and Interfacial shear strength, ISS for all reaction conditions.

Sample	Average fiber critical length, L_c (mm)	Interfacial shear strength, ISS[a] (MPa)
M0.0	8.43 ± 1.85	3.5 ± 0.8
M1.0	4.10 ± 0.64	7.4 ± 1.1
M1.5	4.94 ± 1.19	5.8 ± 1.4
M2.0	4.49 ± 0.34	6.5 ± 0.5

[a] Calculated from Eq. (1).

small tensile tester (Minimat, by Polymer Laboratories), equipped with a thermostatic chamber, and located under a polarized optical stereo-microscope (Wild M3Z by Leica). At least seven samples were tested for each experimental condition. All samples were loaded up to a strain of 10% in order to ensure the saturation of the fragmentation process. The mean fiber length, L_s, was measured by means of an image analyzer system, as proposed by Ohsawa et al. [35].

3.4. Morphological characterization

The effectiveness of PP in situ polymerization, as well as the morphological features of fibers surface and microcomposites subjected to mechanical tests, was studied by SEM. A JEOL 35 CF microscope, equipped with secondary electron detection and X-ray disperse energy microanalysis EDAX DX4 was used. The EDX spectra give the elemental analysis of a 1 μm^2 area. All the samples were previously coated with Au in a vacuum chamber. In the case of microcomposites, cryogenic fracture surfaces were obtained after the fragmentation. Ten samples were used for each reaction condition and microcomposite fracture analysis. The samples were explored and ten micrographs/spectra were taken for each sample.

4. Results and discussion

4.1. In situ polymerization

SEM micrographs and EDX spectra for untreated fibers and MAO-treated fibers are reported in Fig. 3. Untreated glass fiber show the typical smooth surface whose EDX spectrum contains Si, Al, Mg, Ca, O and traces of C. In order to check for any possible deterioration of the fibers caused by the surface treatment, a set of fibers were subjected only to MAO pretreatment. In fact, this represents the most aggressive chemical agent for glass among those used for the surface treatment. The results are shown in Fig. 3b. It can be observed that Al/O ratio increases with respect to the pure fiber, but no appreciable damages can be detected on the fiber. A grey metallic brightness can be noticed by naked eye, indicating that a fine Al layer is uniformly coating the fiber surface.

In a previous work [30], a set of screening experiments was performed to prove the occurrence of a surface polymerization reaction. Two hydroxy-α-olefin concentrations were explored, 0.4% and 4%. In both cases PP chains remained grafted onto the glass surface, even after the physically bonded polymer was eliminated by a solvent extraction treatment. Different morphologies of the grafted polymer resulted at low or high 9 decen-1-ol concentrations, respectively. In the present work, the range of hydroxy-α-olefin concentrations was chosen in view of these results and taking into account that the catalyst activity drastically decreases with the hydroxy-α-olefin concentration.

Fig. 4 show the fibers after in situ polymerization for all the hydroxy-α-olefin concentrations used. The EDX spectra are also included to verify the nature of the species attached to the fibers and to bring a rough estimation of their relative amount. Please note that the peak at 2.12 corresponds to the Au conductive coating layer.

For all the hydroxy-α-olefin concentrations, polymer attached to the fibers appears as white particles in the SEM micrographs. From EDX spectra, it is clear that the C peak notably increases after surface polymerization. As the hydroxy-α-olefin concentration increases, it seems to be an optimum in the amount of PP polymerized onto the fibers. Also, this fact emerges by comparing either the micrographs or the relative area of C to Si peaks. The optimum is reached at 1.0% of hydroxy-α-olefin as shown in Fig. 4b. Two micrographs at different magnifications (400× and 2000×) are included in this figure in order to give a better idea of the complete coverage of the fiber by the polymer.

4.2. Fiber strength

Tensile tests on both untreated and MAO treated single glass fibers were performed to determine their strength. The average diameter of the untreated fibers resulted to be 26.8 ± 1.8 μm, while those of MAO treated fibers was 25.1 ± 1.0 μm. The strength data were statistically treated according to the Weibull distribution. The results are summarized in Fig. 5. It is worth to note that the MAO treatment induces only a slight decrease in the fiber tensile strength as documented by the small reduction in the Weibull scale parameter, σ_0, reported in Table 1. At the same time, a slight increase of the Weibull shape parameter, m, accounts for a somewhat sharper distribution of strength values of the treated fibers around an average value. These results are in agreement with the morphological observations reported above and provide further evidence that MAO treatment does actually induce very limited fiber damage. Anyway, the effects of this small reduction of the fiber strength on the interfacial adhesion have been taken into account by considering the actual values of the fiber strength at the critical length.

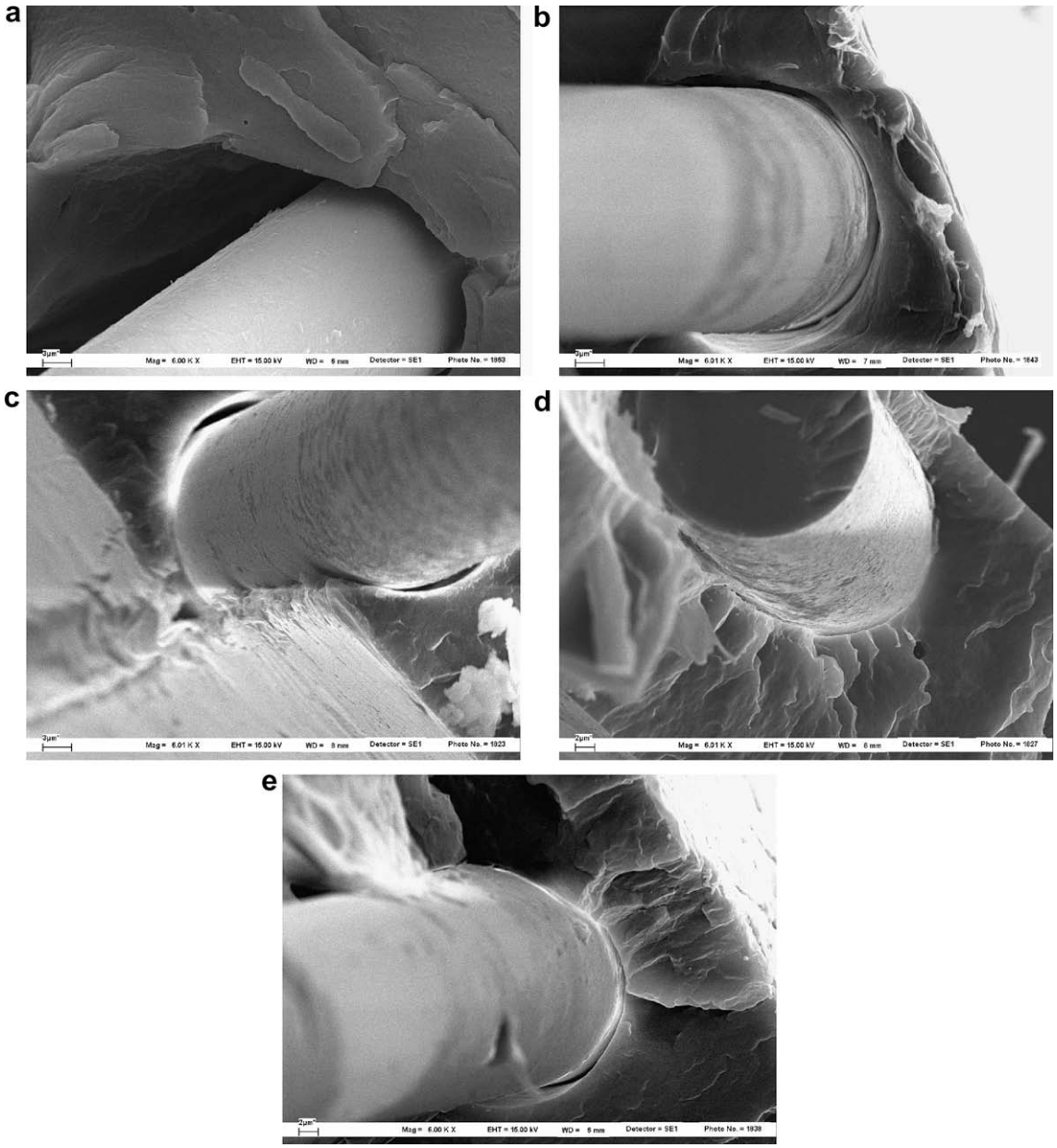

Fig. 7. SEM microphotographs (6000×) from cryogenic fracture surface of different microcomposite samples: (a) M0.0, (b) M0.5, (c) M1.0, (d) M1.5, and (e) M2.0.

4.3. Interfacial adhesion

Fragmentation experiments were performed on model composites consisting of a single fiber embedded in a polymeric matrix. An example of the fiber failure appearance is reported in Fig. 6 for M0.0 and M1.0. For the untreated fibers (Fig. 6a), the interfacial debonding appear to be the dominant failure mechanism thus indicating low-adhesion condition. On the other side, a different failure behavior is observed for microcomposites with fibers previously treated with 1.0% of hydroxy-α-olefin. Here, a radial matrix crack or mixed radial-conical cracks are occurring (Fig. 6b). This behavior is an indication of a somewhat better fiber matrix-adhesion, as it was reported by Pegoretti et al. [7]. From Fig. 6 it also clearly emerges that the number of fiber fragments increases with the interfacial adhesion, resulting in a shorter critical length, as summarized in Table 2. In the same Table, the interfacial shear strength, calculated in accordance to Eq. (1), is also reported. The adhesion markedly increases when fibers with in situ polymerization are considered. For microcomposites obtained with fibers in situ polymerized by using 1.0% of hydroxy-α-olefin, an ISS value more than two times higher than that of the untreated fibers is observed. On the other hand, it appears that the improvement of interfacial adhesion decreases as the amount of hydroxy-α-olefin used in polymerization decreases. This behavior could be explained in terms of a competition between the length of the growing PP chains and the number of anchorage points generated on the fiber surface. In fact, the higher the amount of hydroxy-α-olefin, the higher the number of anchorage points and the lower the PP chain length. The anchorage is formed by the reaction between the hydroxyl groups of the hydroxy-α-olefin and the aluminoxane from MAO, which is bonded to the glass surface [30,31]. Then, as the hydroxy-α-olefin concentration increases, the number of anchorage points also increases. However, the presence of hydroxy-α-olefin (a polar compound) results in a decrease of the catalyst's activity. Aaltonen et al. [36,37] showed that the synthesis of hydroxyl group containing polyolefins with metallocene/methylaluminoxane

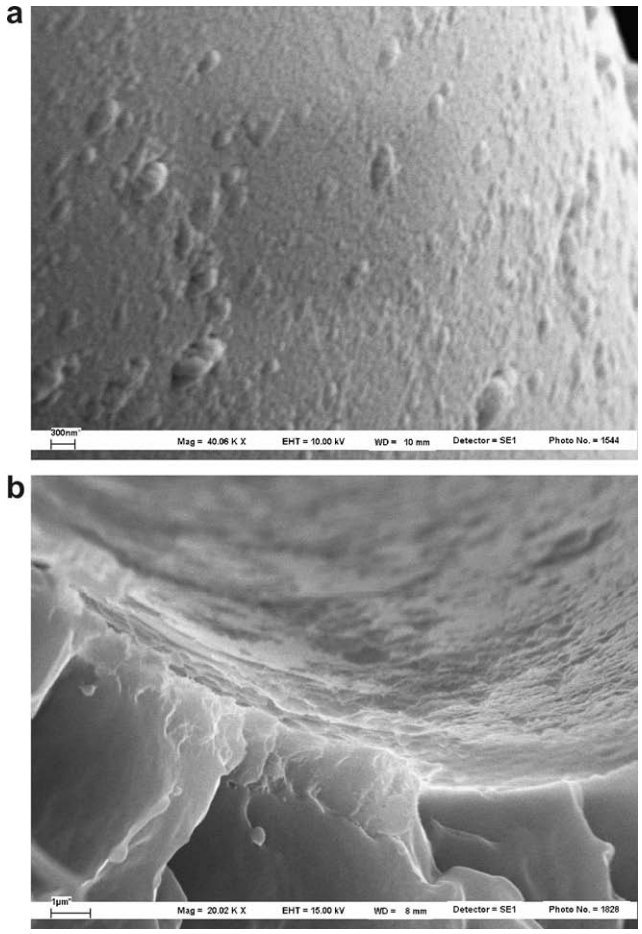

Fig. 8. SEM microphotographs from cryogenic fracture surface of (a) fiber M1.0 (40,000×) and (b) interface M1.5 (20,000×).

catalysts displayed a polymerization rate with decay type kinetics. In particular, these authors reported that an increase of hydroxy-α-olefin concentration reduced the consumption rate of propylene when the other polymerization conditions were kept constant. So, it appears from their results that the PP chain length between anchorage points decreases with the hydroxy-α-olefin concentration. Since interfacial adhesion is developed mostly by PP molecular entanglements, the incidence of chain lengths should be more important than the number of anchorage points.

4.4. Microcomposites interface characterization

After the fragmentation test, the morphology of cryogenically obtained fracture surfaces of microcomposites was analyzed by SEM. Fig. 7 shows the appearance of both untreated and treated samples with different concentrations of hydroxy-α-olefin, as observed at 6000× magnifications. For the sample M0.0, the neat fiber pull-out and the absence of polymer attached to the fiber surface are clearly indicating a very limited adhesion between PP and fiber (Fig. 7a). On the other hand, the fracture surfaces of microcomposites made with in situ polymerized fibers shows features indicating a better fiber–matrix adhesion. In fact, as documented in Fig. 7b–e, PP partially adheres to the fiber surface. Fig. 8 also shows, but at higher magnification, that PP is adhered to the fiber surface of M1.0 and M1.5 samples. The increment in adhesion is also demonstrated by the radial fracture cracks emanating from the fiber interface (Figs 7d and e and 8b). This latter feature indicates that the PP–glass interface strength is more stable than PP–PP entanglements and the fracture occurs in the PP region around the fibers, not at the interface.

5. Conclusions

The technique of in situ metallocenic polymerization of propylene onto the glass fibers surface resulted to be a promising route to increase the adhesion between PP matrix and GF reinforcement since an enhanced compatibility between them can be obtained.

In particular, on the basis of the experimental data generated in this work, the following conclusions can be drawn:

- The amount of PP polymerized onto the fiber and the interfacial adhesion seems to be optimal for 1.0% of hydroxy-α-olefin addition.
- The interfacial shear strength of PP–GF composites, measured by the fragmentation test, was considerably improved (up to a factor of 2.1) with respect to the case of untreated fiber-PP composites.
- The observation of cryogenic fracture surface of microcomposites corroborates the above conclusions since the polymer remained attached to the fiber surface for the samples subjected to polymerization.

Acknowledgments

Travel expenses of collaborating parties were partly covered by the Ministerio de Educación, Ciencia y Tecnología of Argentina and by the Ministero degli Affari Esteri of Italy under the Joint Program on Scientific and Technological Cooperation for years 2006–2007. Financial support from CONICET (Consejo Nacional de Investigaciones Científicas) and ANPCyT (Agencia Nacional de Promoción Científica y Tecnológica) are acknowledged.

References

[1] Yosoyima R, Morimoto K, Susuki T, Nakajima A, Ikada Y. Adhesion and bonding in composites. New York: Marcel Dekker; 1990.
[2] DiBenedetto AT. Tailoring of interfaces in glass fiber reinforced polymer composites: a review. Mater Sci Eng A 2001;302:74–82.
[3] Mallick PK. Fiber reinforced composites. Materials, manufacturing and design. New York: Marcel Dekker; 1997.
[4] Karger-Kocsis J. Polypropylene: structure, blends and composites. Composites, vol. 3. London: Chapman & Hall; 1994.
[5] Xantos M. Functional fillers for plastics, part II. Molenbach, Germany: Wiley; 2005.
[6] Accorsi ML, Pegoretti A, DiBenedetto AT. Dynamic analysis of fibre breakage in single- and multiple-fibre composites. J Mater Sci 1996;31:4181–7.
[7] Pegoretti A, Accorsi ML, DiBenedetto AT. Fracture toughness of the fibre-matrix interface in glass-epoxy composites. J Mater Sci 1996;31:6145–53.
[8] Herrera-Franco PJ, Drzal LT. Comparison of methods for the measurements of fibre/matrix adhesion in composites. Composites 1992;23:2–27.
[9] Narkis M, Chen JH. Review of methods for characterization of interfacial fibre–matrix interactions. Polym Compos 1988;9:245–51.
[10] Kim JK, Mai YW. Engineered interfaces in fiber reinforced composites. Oxford: Elsevier; 1998.
[11] Pegoretti A, Fambri L, Migliaresi C. Interfacial stress transfer in nylon-6/E-glass microcomposites: effect of temperature and strain rate. Polym Compos 2000;21:466–75.
[12] Kelly A, Tyson WR. Tensile properties of fibre-reinforced metals. J Mech Phys Solids 1965;13:329–50.
[13] Fraser AA, Ancker FH, DiBenedetto AT. A computer modelled single filament technique for measuring coupling and sizing agent effects in fibre reinforced composites. In: Proceedings of 30th SPE-ANTEC, Washington DC, USA, Paper 22-A; 1975. p. 1–13.
[14] DiBenedetto AT. Measurement of the thermomechanical stability of interphases by the embedded single fiber test. Compos Sci Technol 1991;42:103–23.
[15] Feillard P, Désarmont G, Favre JP. A critical assessment of the fragmentation test for glass/epoxy systems. Compos Sci Technol 1993;49:109–19.
[16] Feillard P, Désarmont G, Favre JP. Theoretical aspects of the fragmentation test. Compos Sci Technol 1994;50:265–79.

[17] Broutman, LJ. Measurement of the fiber-polymer matrix interfacial strength. In: Interfaces in composites, ASTM STP 452, American Society for Testing and Materials; 1969. p. 27–41.
[18] Penn LS, Lee SM. Interpretation of experimental results in the single pull-out filament test. Compos Technol Res 1989;11:23–30.
[19] Chua PS, Piggot MR. The glass fibre–polymer interface: II-Work of fracture and shear stresses. Compos Sci Technol 1985;22:107–19.
[20] Miller B, Muri P, Rebenfeld L. A microbond method for determination of the shear strength of a fiber/resin interface. Compos Sci Technol 1987;28:17–32.
[21] Gaur U, Miller B. Microbond method for determination of the shear strength of a fiber/resin interface: Evaluation of experimental parameters. Compos Sci Technol 1989;34:35–51.
[22] Wagner HD, Gallis HE, Wiesel E. Study of the interface in Kevlar 49-epoxy composites by means of microbond and fragmentation test: effect of materials and testing variables. J Mater Sci 1993;28:2238–44.
[23] Mandell JF, Grande DH, Tsiang TH, McGarry FJ. Modified microdebonding test for direct In situ fiber/matrix bond strength determination in fiber composites. In: Whithney JM, editor. Proceedings of the 7th conference composite materials: testing and design, ASTM STP 893, Philadelphia; 1986. p. 87–108.
[24] Desaenger M, Verpoest I. On the use of the micro-indentation test technique to measure the interfacial shear strength of fibre-reinforced polymer composites. Compos Sci Technol 1993;48:215–26.
[25] Kalinka G, Leistner A, Hampe A. Characterization of the fibre/matrix interface in reinforced polymers by the push-in technique. Compos Sci Technol 1997;57:845–51.
[26] Drzal LT, Herrera-Franco P. Composite fibre–matrix bond test. In: Engineered materials handbook: adhesives and sealants, vol. 3, Materials Park, (OH): ASM International; 1991.
[27] Weibull W. A statistical distribution function of wide applicability. J Appl Mech ASME 1951;18:293–7.
[28] Asloun EM, Donnet JB, Guilpan G, Nardin M, Schultz J. On the estimation of the tensile strength of carbon fibres at short lengths. J Mater Sci 1989;24:3504–10.
[29] Gurvich MR, DiBenedetto AT, Pegoretti A. On evaluation of the statistical parameters of a Weibull distribution. J Mater Sci 1997;32:3711–6.
[30] Barbosa S, Ferreira ML, Damiani D, Capiati N. Copolymerization of polypropylene and funcionalized linear α-olefin onto glass fibers. J Appl Polym Sci 2001;81:1266–76.
[31] Etcheverry M, Damiani D, Ferreira ML, Barbosa S, Capiati N. Chemical grafting of metallocene-catalyzed functional polypropylene copolymer on glass substrates through surface modification. J Appl Polym Sci 2007;109:2815–22.
[32] Paiva MC, Bernardo CA, Nardin M. Mechanical, surface and interfacial characterization of pitch and PAN based carbon fibres. Carbon 2000;38:1323–37.
[33] ASTM D3379, 1975 (reapproved 1989).
[34] Villar M, Ferreira ML. Co- and terpolymerization of ethylene, propylene, and higher α-olefins with high propylene contents using metallocene catalysts. J Polym Sci A 2001;39:1136–48.
[35] Ohsawa T, Nakayama A, Miwa M, Hasegawa A. Temperature dependence of critical fiber length for glass fiber-reinforced thermosetting resins. J Appl Polym Sci 1978;22:3203–12.
[36] Aaltonen P, Fink G, Löfgren B, Seppala J. Synthesis of hidroxyl group containing polyolefins with metallocene/methilaluminoxane catalysts. Macromolecules 1996;29:5255–60.
[37] Aaltonen P, Löfgren B. Functionalization of polyethylenes via metallocene/methilaluminoxane catalyst. Eur Polym J 1997;33:1187–90.